

Quantum critical behavior in heavy-fermion superconductor CeIrIn₅

S. Kambe, H. Sakai, and Y. Tokunaga

Advanced Science Research Center, Japan Atomic Energy Agency, Tokai, Ibaraki 319-1195, Japan

R. E. Walstedt

Physics Department, The University of Michigan, Ann Arbor, MI 48109, USA

(Received 15 August 2010; revised manuscript received 16 September 2010; published 7 October 2010)

Based on analysis of nuclear (¹¹⁵In) spin-lattice relaxation-time measurements on the heavy-fermion superconductor CeIrIn₅, \vec{q} , ω , and temperature dependences of the dynamical susceptibility $\text{Im} \chi(\vec{q}, \omega_n)$ near the antiferromagnetic wave vector \vec{Q} at low energy $\omega_n \sim 10^{-4}$ meV have been estimated. The T dependences found, $\text{Im} \chi(\vec{Q}, \omega_n) \sim T^{-3/2}$ and antiferromagnetic correlation length $\xi \sim T^{-3/4}$, are consistent with quantum critical behavior for a three-dimensional antiferromagnet ($d=3$, $z=2$) having a spin-density-wave instability.

DOI: [10.1103/PhysRevB.82.144503](https://doi.org/10.1103/PhysRevB.82.144503)

PACS number(s): 76.60.-k, 75.30.Mb

I. INTRODUCTION

Since unconventional superconductivity occurs near magnetic quantum critical points (QCPs) in many heavy-fermion systems, the clarification of quantum criticality is one of the crucial issues for its understanding.¹ In heavy-fermion systems CeMIn₅ (M : Co, Rh, and Ir), superconductivity considered to appear in the vicinity of QCP.² In fact, the antiferromagnetic (AFM) ordering which is observed in CeRhIn₅ is suppressed under pressure, and superconductivity appears.³ In paramagnetic CeCoIn₅, a modest amount of chemical pressure (substitution of ligand atoms) causes antiferromagnetic ordering.^{4,5}

Because of the tetragonal crystal structure with Ce occupying a basal plane, the possibility of two-dimensional (2D) magnetic character in CeMIn₅ has been considered. For example, NQR spin-lattice relaxation measurements were said to suggest magnetic fluctuations with quasi-2D character in CeIrIn₅.⁶ In contrast, anisotropic, three-dimensional (3D) magnetic excitations have been reported in CeRhIn₅.⁷ In the present report, the nature and dimensionality of a possible QCP in CeIrIn₅ are considered.

In our previous study,⁸ the dynamical susceptibility of CeIrIn₅ ($T_c \sim 0.4$ K at ambient pressure⁹) was estimated based on spin-lattice relaxation and Knight shift measurements at the In sites. However, the estimated dynamical susceptibility was effectively a \vec{q} -averaged one since the \vec{q} dependence of the hyperfine coupling and the dynamical susceptibility were ignored in the analysis. In antiferromagnetically correlated CeIrIn₅, it is necessary to treat the \vec{q} dependence correctly in order to extract the true dynamical susceptibility, particularly because the antiferromagnetic fluctuations tend to cancel at the In sites.¹⁰ Moreover, the spin-lattice relaxation rate is not related to the dynamical susceptibility in a simple way in CeMIn₅ systems because of the \vec{q} - and T -dependent⁸ hyperfine couplings and dynamical susceptibility.

In the present study the \vec{q} dependence of the hyperfine couplings and of the dynamical susceptibility are taken into account explicitly. In this way the T dependence of the AFM correlation length and of the dynamical susceptibility in CeIrIn₅ are estimated, which indicates that CeIrIn₅ is located

in the vicinity of a 3D AFM quantum critical point.

II. EXPERIMENTAL

Experimental details have been provided in a previous report.⁸ High-quality, single-crystal samples of CeIrIn₅ have been prepared by the Czochralski method.¹¹ NMR measurements on the ¹¹⁵In nuclear spins ($I=9/2$, gyromagnetic ratio $\gamma_n=9.3295$ MHz/T) were carried out using a phase coherent pulsed spectrometer. In this HoCoGa₅($I4/mmm$)-structure compound, having lattice parameters $a=4.666$ Å and $c=7.5168$ Å (Ref. 12) (Fig. 1), there are two crystallographically inequivalent In sites: the $1c$ site [In(1)] and the $4i$ site [In(2)]. The In(1) site has tetragonal local symmetry while the In(2) site is orthorhombic. The Knight shift K and spin-lattice relaxation time T_1 have been determined at both of the ¹¹⁵In sites in a single crystal CeIrIn₅ as a function of temperature and applied magnetic field orientation ($H \parallel a, c$ axes). The Knight shift has been determined using field-sweep

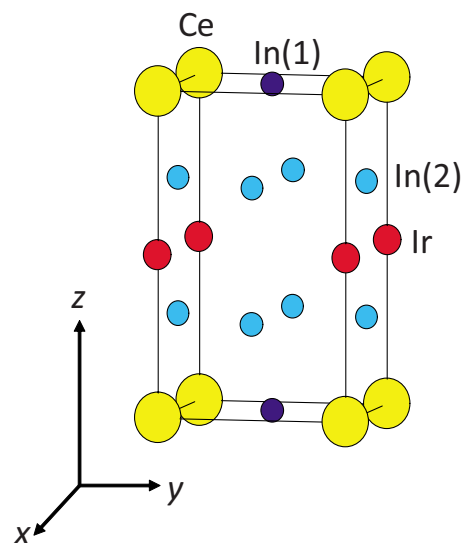


FIG. 1. (Color online) Crystal structure ($I4/mmm$) of CeIrIn₅. There are two crystallographically inequivalent In sites, the $1c$ site [In(1)] and the $4i$ site [In(2)].

spectra taken at constant frequency $\omega_n/2\pi=59.8$ MHz. T_1 data were obtained using the standard spin-echo inversion recovery method at $\omega_n/2\pi\sim 75$ MHz.

III. RESULTS AND DISCUSSION

A. Spin-lattice relaxation and dynamical susceptibility

Generally, the spin-lattice relaxation time T_1 can be expressed as¹³

$$1/T_1 T_{H||k} = \gamma_n^2 \sum_{\vec{q}} \left\{ A_l(\vec{q})^2 \frac{\text{Im} \chi_l(\vec{q}, \omega_n)}{\omega_n} + A_m(\vec{q})^2 \frac{\text{Im} \chi_m(\vec{q}, \omega_n)}{\omega_n} \right\}, \quad (1)$$

where l and m axes are perpendicular to k axis, $A(\vec{q})$ is the $\vec{q} \equiv (q_x, q_y, q_z)$ -dependent hyperfine coupling constant, $\text{Im} \chi(\vec{q}, \omega_n)$ is the dynamical susceptibility, ω_n is the NMR measurement frequency, and $\sum_{\vec{q}}$ is a normalized sum over the Brillouin zone (BZ).

Single-axis relaxation rate contributions $R_{i,\alpha}$ for each In site $i(=1, 2)$ and fluctuation axis $\alpha(=a, c)$ may be defined by

$$R_{i,\alpha} = \gamma_n^2 \sum_{\vec{q}} A_{i,\alpha}(\vec{q})^2 \frac{\text{Im} \chi_{i,\alpha}(\vec{q}, \omega_n)}{\omega_n}. \quad (2)$$

Combining Eqs. (1) and (2), comprehensive spin-lattice relaxation rate data may then be analyzed to yield the T dependences of the single-axis rates $R_{i,\alpha}$. Data for the latter quantities can then be further analyzed to yield experimental values for weighted averages of the dynamical susceptibility over the BZ. To see this we define $A_{i,\alpha}(\vec{q})^2 = A_{i,\alpha}(0)^2 |f_i(\vec{q})|^2$, where $|f_i(\vec{q})|^2$ is the hyperfine form factor. Equation (2) can then be rewritten as

$$\begin{aligned} R_{i,\alpha} &= \gamma_n^2 A_{i,\alpha}(0)^2 \sum_{\vec{q}} |f_i(\vec{q})|^2 \frac{\text{Im} \chi_{i,\alpha}(\vec{q}, \omega_n)}{\omega_n} \\ &= \gamma_n^2 A_{i,\alpha}(0)^2 \frac{\overline{\text{Im} \chi_{i,\alpha}(\vec{q}, \omega_n)}}{\omega_n}, \end{aligned} \quad (3)$$

where we define

$$\overline{\text{Im} \chi_{i,\alpha}(\vec{q}, \omega_n)} \equiv \sum_{\vec{q}} |f_i(\vec{q})|^2 \text{Im} \chi_{i,\alpha}(\vec{q}, \omega_n).$$

In CeIrIn₅ the hyperfine coupling constants $A_{i,\alpha}(0)$, which have been determined with K - χ plots, have been found to be T dependent at low temperatures.⁸

Experimentally derived values of $\overline{\text{Im} \chi_{2,\alpha}(\vec{q}, \omega_n)}$ obtained via Eq. (3) are plotted as a function of temperature in Fig. 2. The source of magnetic fluctuations at the In sites is transferred hyperfine coupling from neighboring Ce moments. These moments also give rise to the dynamical susceptibility $\text{Im} \chi_{i,\alpha}(\vec{q}, \omega_n)$. Therefore, $\text{Im} \chi_{1,\alpha}(\vec{q}, \omega_n)$ should be identical with $\text{Im} \chi_{2,\alpha}(\vec{q}, \omega_n)$. However, estimated values of $\overline{\text{Im} \chi_{1,\alpha}(\vec{q}, \omega_n)}$ deviate notably from those of $\overline{\text{Im} \chi_{2,\alpha}(\vec{q}, \omega_n)}$, especially at low temperatures. As is shown below, these deviations can be understood in terms of the different

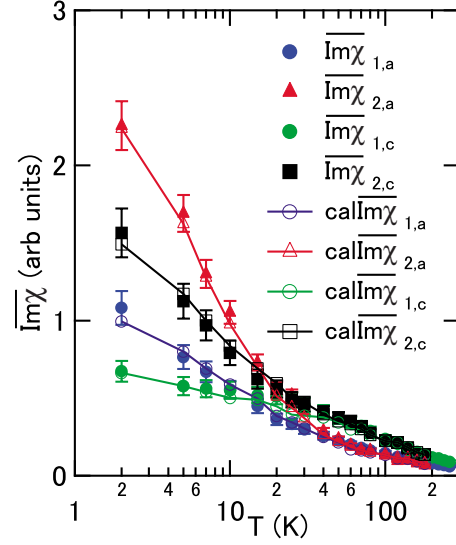


FIG. 2. (Color online) T dependence of the \vec{q} -summated dynamical susceptibility $\text{Im} \chi_{i,\alpha}(\vec{q}, \omega_n)$ in CeIrIn₅ (Ref. 8) [$i=1$ and 2 for the In(1) and In(2) sites, and $\alpha=a$ and c for the a and c axes, respectively]. Values of $\text{cal Im} \chi_{i,\alpha}(\vec{q}, \omega_n)$ are calculated based on Eq. (7), using ξ_{xy} and $\text{Im} \chi_{\alpha}(\vec{Q}, \omega_n)$ values from Figs. 7 and 8 (see Sec. III C). The solid lines are guide to the eyes.

\vec{q} -dependent hyperfine form factors for the two In sites, where we also model and obtain estimates of the \vec{q} dependence of the dynamical susceptibility and the temperature variation in the magnetic correlation length.

B. \vec{q} -dependent hyperfine coupling and dynamical susceptibility

In Fig. 3, Ce ions which neighbor the In(1) and In(2) sites are shown. The Ce ions are the source of transferred hyperfine fields at the In sites.

Considering the four nearest-neighbor Ce ions, the \vec{q} dependence of $|f_1(\vec{q})|^2$ for the In(1) site can be written as

$$|f_1(\vec{q})|^2 = 4 \cos^2(\pi q_x) \cos^2(\pi q_y), \quad (4)$$

where $\sum_{\vec{q}} |f_1(\vec{q})|^2 = 1$. The resulting \vec{q} dependence of the form factor $|f_1(\vec{q})|^2$ over the BZ is illustrated in Fig. 4.¹⁴

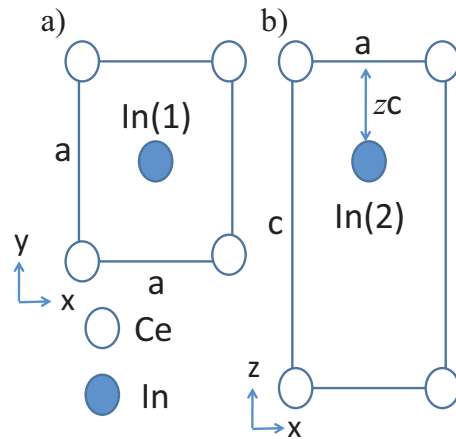


FIG. 3. (Color online) Ce sites included in the \vec{q} -dependent hyperfine coupling. (a) Nearest-neighbor Ce sites around the In(1) site. (b) Nearest- and second-neighbor Ce sites around the In(2) site.

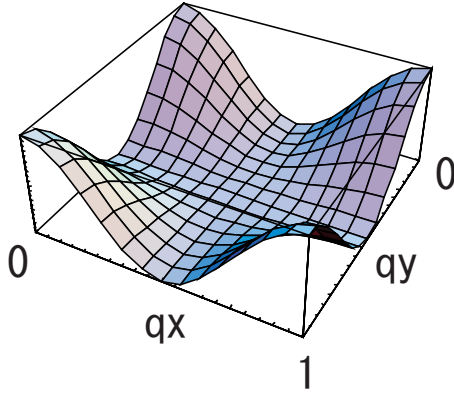


FIG. 4. (Color online) \vec{q} dependence of the In(1)-site hyperfine form factor $|f_1(\vec{q})|^2$ for values of \vec{q} surrounding the planar AFM wave vector $(q_x, q_y) = (\frac{1}{2}, \frac{1}{2})$.

For the In(2) site, the \vec{q} dependence of $|f_2(\vec{q})|^2$ can be written approximately considering two nearest and two second-nearest Ce sites (see Fig. 5),

$$|f_2(\vec{q})|^2 = 4 \cos^2(\pi q_x) \times \{B_1 \cos(2\pi q_z) + B_2 \cos[2\pi q_z(1-z)]\}^2 + \{B_1 \sin(2\pi q_z) - B_2 \sin[2\pi q_z(1-z)]\}^2, \quad (5)$$

where $z=0.305$ is the z parameter of the crystal structure.¹² B_1/B_2 is the ratio of hyperfine coupling constants for the nearest and second nearest-neighbor sites. If the hyperfine coupling is assumed to be the Ruderman-Kittel-Kasuya-Yoshida type, B_1/B_2 is estimated as $\sim (r_1/r_2)^3 \approx 5$, where r_1 and r_2 are the distances between first- and second-neighbor Ce ions and the In(2), respectively. The values of $B_1=0.60$ and $B_2=0.12$ are then chosen so that $\sum_{\vec{q}} |f_2(\vec{q})|^2 = 1$.

Since the magnetic correlation wave vector is near $\vec{Q} = (\frac{1}{2}, \frac{1}{2}, \frac{1}{2})$ in related compounds CeRhIn₅ (Ref. 15) (exactly, under pressure above 1.7 GPa near the superconducting state) and CeCoIn₅,¹⁶ we assume that the magnetic correlation wave vector in CeRhIn₅ is \vec{Q} as well. Then, the \vec{q} dependence of $\text{Im} \chi_\alpha(\vec{q}, \omega_n)$ in the vicinity of the antiferromagnetic wave vector \vec{Q} can be approximated as

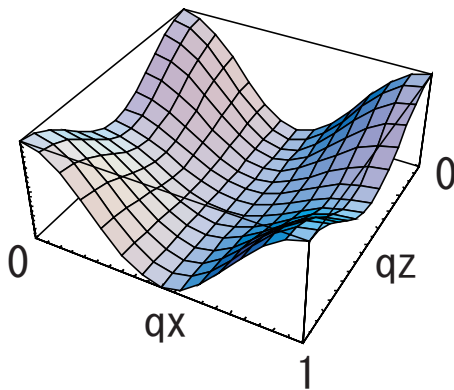


FIG. 5. (Color online) \vec{q} dependence of hyperfine form factor $|f_2(\vec{q})|^2$ near the antiferromagnetic wave vector $(q_x, q_z) = (\frac{1}{2}, \frac{1}{2})$ affecting the In(2) site.

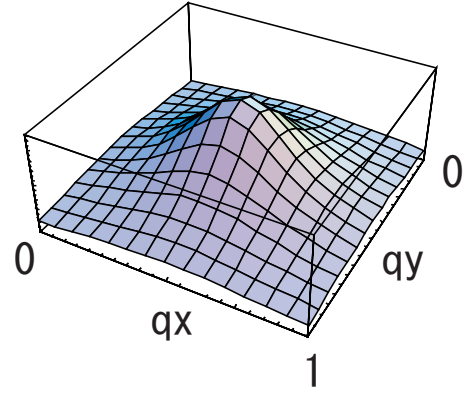


FIG. 6. (Color online) \vec{q} dependence of the dynamical susceptibility $\text{Im} \chi_\alpha(\vec{q}, \omega_n)$ near the AFM wave vector $(q_x, q_y) = (\frac{1}{2}, \frac{1}{2})$ for the case of $\xi_{xy}=4$.

$$\text{Im} \chi_\alpha(\vec{q}, \omega_n) \approx \text{Im} \chi_\alpha(\vec{Q}, \omega_n) \left[1 + \left\{ \xi_{xy} \left(q_x - \frac{1}{2} \right) \right\}^2 + \left\{ \xi_{xy} \left(q_y - \frac{1}{2} \right) \right\}^2 + \left\{ \xi_z \left(q_z - \frac{1}{2} \right) \right\}^2 \right]^{-1}, \quad (6)$$

where ξ_{xy} (in units of a) and ξ_z (in units of c) are the antiferromagnetic correlation lengths in the basal plane and along the z axis, respectively. As discussed above, the actual $\text{Im} \chi_\alpha(\vec{q}, \omega_n)$ should be the same for both In sites. For example, \vec{q} dependence of $\text{Im} \chi_\alpha(\vec{q}, \omega_n)$ for $\xi_{xy}=4$ is presented in Fig. 6. If the latter profile is compared with $|f_1(\vec{q})|^2$ in Fig. 4, the cancellation of antiferromagnetically correlated fluctuations is easily understood.

C. T dependence of magnetic correlation length and dynamical susceptibility at \vec{Q}

Based on Eqs. (4)–(6), the T dependence of $\overline{\text{Im} \chi_{i,\alpha}(\vec{q}, \omega_n)}$ becomes

$$\overline{\text{Im} \chi_{i,\alpha}(\vec{q}, \omega_n)} \approx \text{cal} \overline{\text{Im} \chi_{i,\alpha}(\vec{q}, \omega_n)} \equiv \text{Im} \chi_\alpha(\vec{Q}, \omega_n) \times \sum_{\vec{q}} |f_i(\vec{q})|^2 \left[1 + \left\{ \xi_{xy} \left(q_x - \frac{1}{2} \right) \right\}^2 + \left\{ \xi_{xy} \left(q_y - \frac{1}{2} \right) \right\}^2 + \left\{ \xi_z \left(q_z - \frac{1}{2} \right) \right\}^2 \right]^{-1}. \quad (7)$$

Since the critical exponent ν for the correlation length ($\xi \propto T^{-\nu}$) is to be same for ξ_{xy} and ξ_z in the paramagnetic state,¹⁷ ξ_{xy}/ξ_z should be independent of T . Further, if ξ_{xy}/ξ_z is taken to be fixed at the value determined near $\omega \approx 0$ for CeRhIn₅, i.e., $\xi_{xy}/\xi_z=4$,⁷ then the T dependences of $\text{Im} \chi_\alpha(\vec{Q}, \omega_n)$ and ξ_{xy} can be determined so as to reproduce the T dependence of $\overline{\text{Im} \chi_{i,\alpha}(\vec{q}, \omega_n)}$. Since a similar value $\xi_{xy}/\xi_z \approx 1.5 \times (c/a) \sim 2.5$ is also found in CeCoIn₅,¹⁶ the presently assumed value $\xi_{xy}/\xi_z=4$ is reasonable.

Figures 7 and 8 show the T dependences of ξ_{xy} and $\text{Im} \chi_\alpha(\vec{Q}, \omega_n)$, which reproduce the T dependences of the

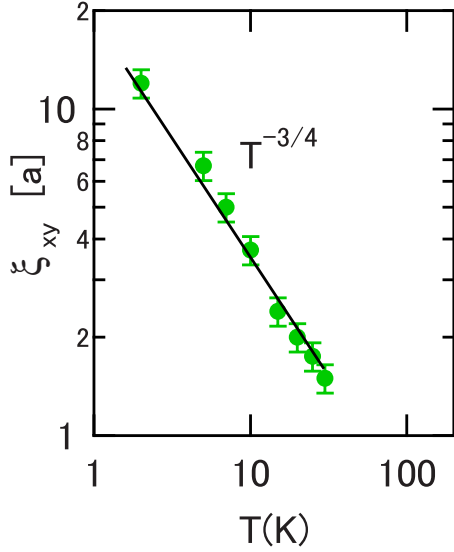


FIG. 7. (Color online) T dependence of the magnetic correlation length in the basal plane ξ_{xy} in unit of $a=4.666$ Å. The estimated T dependence $\xi \sim T^{-3/4}$ is expected for the quantum critical regime of a 3D antiferromagnet ($d=3$, $z=2$).

$\overline{\text{Im}} \chi_{i,\alpha}(\vec{q}, \omega_n)$ (cal $\overline{\text{Im}} \chi_{i,\alpha}(\vec{q}, \omega_n)$ in Fig. 2). As shown in Fig. 2, the deviations between $\text{Im} \chi_{1,\alpha}(\vec{q}, \omega_n)$ and $\text{Im} \chi_{2,\alpha}(\vec{q}, \omega_n)$ can be reproduced within the experimental errors.

If the \vec{q} dependence of hyperfine form factor at the In(1) was different from the real one in Fig. 4; (a) \vec{q} -independent case: $|f_1(\vec{q})|^2=1$ and (b) cancellation at $\vec{q}=(0,0)$ case: $|f_1(\vec{q})|^2=|f_a(\vec{q})|^2 \equiv 4 \sin^2(\pi q_x) \sin^2(\pi q_y)$ (Fig. 9), T dependence of cal $\overline{\text{Im}} \chi_{1,a}(\vec{q}, \omega_n)$ using the obtained ξ_{xy} and $\text{Im} \chi_a(\vec{Q}, \omega_n)$ would be considerably different from the observed $\text{Im} \chi_{1,a}(\vec{q}, \omega_n)$ (\approx cal $\overline{\text{Im}} \chi_{1,a}(\vec{q}, \omega_n)$ for the real $|f_1(\vec{q})|^2$ in Fig. 4), as shown in Fig. 10. This fact indicates

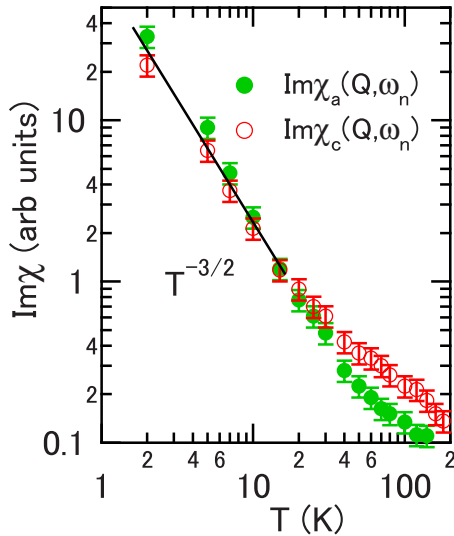


FIG. 8. (Color online) T dependence of the dynamical susceptibility $\text{Im} \chi_a(\vec{Q}, \omega_n)$ at AFM wave vector $\vec{Q}=(\frac{1}{2}, \frac{1}{2}, \frac{1}{2})$. It should be noted that the vertical unit is the same as in Fig. 2. The estimated T dependence $\text{Im} \chi_a(\vec{Q}, \omega_n) \sim T^{-3/2}$ is expected for the quantum critical regime of a 3D antiferromagnet ($d=3$, $z=2$).

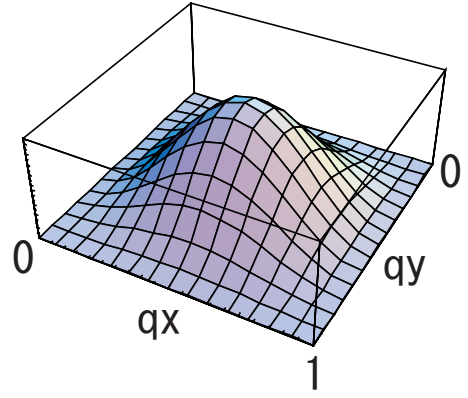


FIG. 9. (Color online) \vec{q} dependence of hyperfine form factor $|f_a(\vec{q})|^2 \equiv 4 \sin^2(\pi q_x) \sin^2(\pi q_y)$ for values of \vec{q} surrounding the planar AFM wave vector $(q_x, q_y) = (\frac{1}{2}, \frac{1}{2})$. In this case, fluctuations at $\vec{q}=(0,0)$ are canceled, in contrast to the real one in Fig. 4.

that T dependence of $1/TT_1$ at the In sites depends strongly on the \vec{q} dependence of hyperfine form factor in CeIrIn₅. Evidently, T dependence of $1/T_1T$ is not scaled with the T dependence of dynamical susceptibility at low temperatures, even if the hyperfine coupling constants were T independent.

Above 30 K, ξ is effectively ~ 0 as no deviation is observed, indicating a nearly uncorrelated localized-moment state, which is consistent with the nearly T -independent T_1 behavior observed in this region.⁸ Since ξ_{xy} extends to ~ 12 sites in the basal plane at the lowest temperature, the system is considered to be near a magnetic instability. Values of ξ estimated with neutron scattering in CeRhIn₅ (Ref. 7) are slightly smaller than the present one, perhaps because ξ are determined in neutron scattering at a finite energy effectively larger than $\omega_n \sim 75$ MHz $\approx 3 \times 10^{-4}$ meV.

Theoretically, ξ can be defined in the quantum critical regime of a 3D antiferromagnetic spin-density-wave (SDW) instability,¹⁸

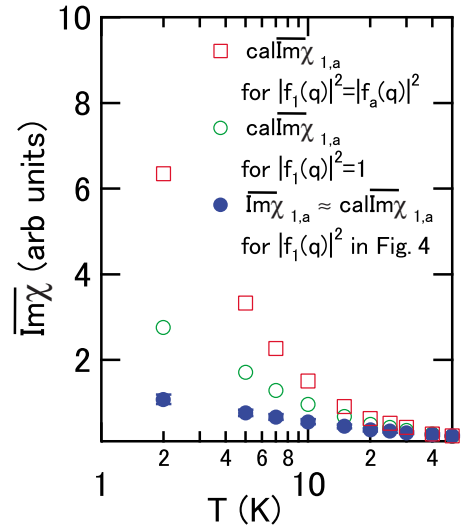


FIG. 10. (Color online) Comparison between the observed $\text{Im} \chi_{1,a}(\vec{q}, \omega_n)$ (shown in Fig. 2) and cal $\overline{\text{Im}} \chi_{1,a}(\vec{q}, \omega_n)$ based on Eq. (7) for the cases of $|f_1(\vec{q})|^2=|f_a(\vec{q})|^2$ and $|f_1(\vec{q})|^2=1$ using the obtained ξ_{xy} (Fig. 7) and $\text{Im} \chi_a(\vec{Q}, \omega_n)$ (Fig. 8). It should be noted that the vertical unit is the same as in Fig. 2.

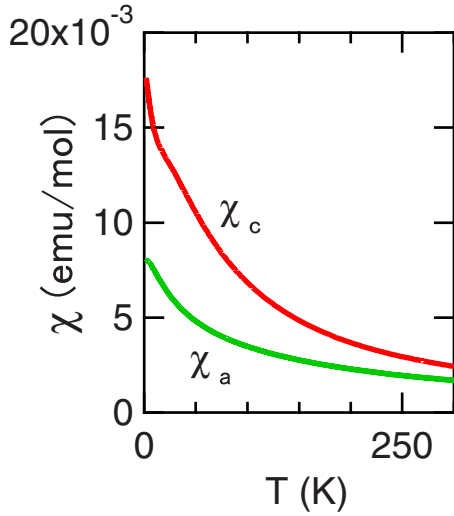


FIG. 11. (Color online) T dependence of the static susceptibility $\chi_\alpha = \chi_\alpha(0,0)$. ($\alpha=a$ for $H\parallel a$ and $\alpha=c$ for $H\parallel c$) (Ref. 11).

$$\xi \sim \chi(\vec{Q},0)^{1/2} \sim T^{-3/4}, \quad (8)$$

where $\chi(\vec{Q},0)$ is the static susceptibility at $q=\vec{Q}$. As shown in Fig. 7, $\xi_{xy} \sim T^{-3/4}$ is observed in CeIrIn₅. Although a quasi-2D scenario is proposed,⁶ the present analysis indicates that CeIrIn₅ is in the 3D antiferromagnetic quantum critical regime below ~ 30 K. Actually, the theoretical expression for T dependence of ξ in a 2D antiferromagnetic quantum critical regime of an itinerant system ($d=z=2$ case) is still controversial.^{19,20} The present analysis is at least consistent with the well-established 3D case, although the magnetic property of CeIrIn₅ is anisotropic.

It should be noted that the estimated critical exponent $\nu \approx 3/4$ for ξ_{xy} is insensitive to a modification of ξ_{xy}/ξ_z value in the vicinity of 4. It is noteworthy that a crossover to 2D behavior for ξ_{xy} can be observed at a finite temperature if $\xi_{xy}/\xi_z \gg 1$, whereas no such behavior is observed before ξ_{xy} becomes zero in the present case.

In the 3D case, quantum critical behavior can be observed roughly below the characteristic spin fluctuation temperature T_0 ,²¹ which is estimated to be ~ 15 K in CeIrIn₅, based on the T dependence of the specific heat.²² Thus, the observation of $\xi_{xy} \sim T^{-3/4}$ below ~ 30 K in the present study is not unexpected.

Figure 8 shows the T dependence of $\text{Im} \chi_\alpha(\vec{Q}, \omega_n)$. In the quantum critical regime for the 3D antiferromagnetic SDW case at $\omega \approx 0$,²¹

$$\text{Im} \chi(\vec{Q},0) \sim \chi(\vec{Q},0) \sim T^{-3/2}. \quad (9)$$

In Fig. 8, the relation $\text{Im} \chi_\alpha(\vec{Q}, \omega_n) \sim T^{-3/2}$ is experimentally confirmed below 30 K, consistent with the 3D behavior of ξ_{xy} .

Because of heavy-fermion enhancement and antiferromagnetic correlations, $\text{Im} \chi_\alpha(\vec{Q}, \omega_n)$ increases strongly compared with $\text{Im} \chi_{i,\alpha}(\vec{q}, \omega_n)$. At high temperatures, $\text{Im} \chi_c(\vec{Q}, \omega_n)$ is larger than $\text{Im} \chi_a(\vec{Q}, \omega_n)$ as the static susceptibility $\chi_c > \chi_a$ presented in Fig. 11,¹¹ however, $\text{Im} \chi_a(\vec{Q}, \omega_n)$ becomes

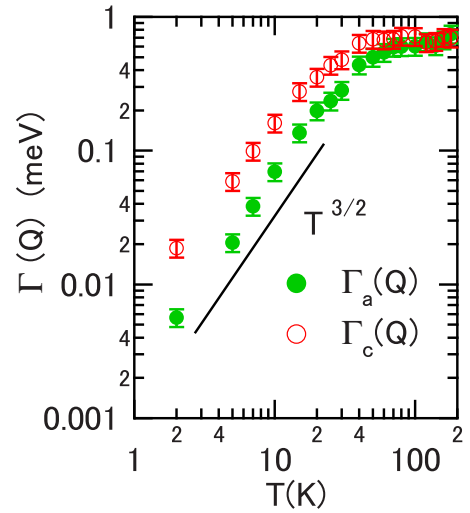


FIG. 12. (Color online) T dependence of the relaxation rate $\Gamma_\alpha(\vec{q})$ at AFM wave vector $\vec{q}=\vec{Q}$. As T is approaching zero, Γ_α seems to approach zero, indicating CeIrIn₅ is in the vicinity of the QCP. The estimated T dependence $\Gamma_\alpha(\vec{Q}) \sim T^{3/2}$ is expected for the quantum critical regime of a 3D AFM ($d=3$, $z=2$).

larger at low temperature, indicating that the system approaches an ordered state with ordered moment in the basal plane. In a similar compound CeRhIn₅, an ordered moment in the basal plane has actually been observed.⁷

The quantum criticality can depend on applied magnetic field. In the present study, however, the spin-lattice relaxation time at the In(1) site at zero field⁶ coincides with our result around $H=8$ T. Therefore, the magnetic field effect is considered to be negligible at least below 8 T.

D. Estimation of relaxation rate $\Gamma_\alpha(\vec{q})$ at $\vec{q}=\vec{Q}$ and the ω dependence of $\text{Im} \chi(\vec{Q}, \omega)$

Using a Lorentzian approximation in terms of the relaxation rate $\Gamma_\alpha(\vec{q})$ at $\vec{q}=\vec{Q}$, the ω dependence of $\text{Im} \chi_\alpha(\vec{Q}, \omega)$ in the region $\omega \sim \omega_n \ll \Gamma_\alpha(\vec{Q})$ can be represented as²³

$$\frac{\text{Im} \chi_\alpha(\vec{Q}, \omega)}{\omega} \approx \frac{\chi_\alpha \Gamma_\alpha(\vec{Q})}{\{\Gamma_\alpha(\vec{Q})^2 + \omega^2\}} \approx \frac{\chi_\alpha}{\Gamma_\alpha(\vec{Q})}, \quad (10)$$

where $\chi_\alpha = \chi_\alpha(0,0)$ is the static susceptibility at $\vec{q}=0$. Based on Eq. (10), the estimated $\text{Im} \chi_\alpha(\vec{Q}, \omega_n)$ (Fig. 8) and the static susceptibility χ_α (Fig. 11), the T dependence of $\Gamma_\alpha(\vec{Q})$ can be evaluated as shown in Fig. 12. As T decreases toward zero, $\Gamma_\alpha(\vec{Q})$ appears to decay toward zero, indicating that the system is in the vicinity of an antiferromagnetic QCP. In the quantum critical regime, $\Gamma(\vec{Q})$ may be expressed as²¹

$$\Gamma(\vec{Q}) \sim \chi(\vec{Q},0)^{-1} \sim T^{3/2}. \quad (11)$$

This relation is in fact confirmed below ~ 30 K.

At high temperatures, $\Gamma_a(\vec{Q}) \approx \Gamma_c(\vec{Q})$ become nearly T independent, indicating that the system is magnetically isotropic without strong correlations. In contrast, at low temperatures, $\Gamma_a(\vec{Q})$ becomes notably smaller than $\Gamma_c(\vec{Q})$. Such a

result is consistent with the conjecture that the system is approaching an antiferromagnetically ordered state with the ordered moment in the basal plane.

In our previous report,²⁴ an approximation for the strongly correlated case was used for estimating \bar{q} summed Γ_α , giving a magnitude similar to the present one.

IV. CONCLUSION

In $CeMIn_5$ systems, nuclear hyperfine couplings at the In sites are strongly T and \bar{q} dependent. The T -dependent hyperfine couplings are found particularly in Ce-based compounds. In contrast, in U- and Np-based isostructural compounds such as $UPtGa_5$ and $NpCoGa_5$, the hyperfine coupling constants are T independent.^{25,26} In the present study, components of the dynamical susceptibility have been estimated with the aid of an analysis of ^{115}In NMR Knight shift and spin-lattice relaxation time results. In particular, we find for the estimated critical behavior: $\xi_{xy} \sim T^{-3/4}$, $\text{Im} \chi_\alpha(\vec{Q}, \omega_n) \sim T^{-3/2}$, and $\Gamma_\alpha(\vec{Q}) \sim T^{3/2}$ as $T \rightarrow 0$. These findings are consistent with 3D quantum critical behavior for a SDW instability.

In Fig. 13, a tentative schematic phase diagram for $CeIrIn_5$ from the present study is presented. It is shown that $CeIrIn_5$ is located in a quantum critical regime below 30 K, and the origin of quantum criticality is suggested to be a 3D antiferromagnetic SDW instability. As $T \rightarrow 0$, the system would approach a QCP, although the appearance of superconductivity prevents us from observing this. Furthermore, no Fermi-liquid regime has been found to appear above the superconducting regime for this compound.⁶ Thus, the quantum critical fluctuations evinced in this study may be relevant to the superconductivity.

In $CeCoIn_5$, $T_c \sim 2.3$ K is almost six times larger than $T_c \sim 0.4$ K in $CeIrIn_5$. Recent NMR studies of $CeCoIn_5$ have suggested 2D magnetic character at low temperatures.²⁸ Of course, a \bar{q} -dependent analysis should be applied to that case, where the correlation between low dimensionality and T_c might be interesting. On the other hand, magnetic fluctuations with XY anisotropy may be favorable for d -wave superconductivity in heavy-fermion systems, as compared with the Ising case.²⁴ In the present study, the XY anisotropy with

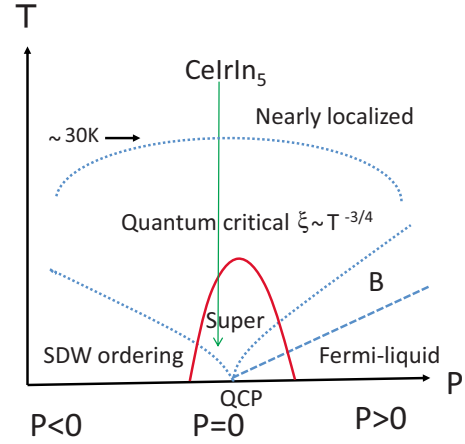


FIG. 13. (Color online) Suggested schematic phase diagram for $CeIrIn_5$. SDW ordering cannot be observed since negative pressure is necessary. Since T_c increases with pressure (Ref. 27), $CeIrIn_5$ may be located on the low-pressure side of the superconducting cone region (red solid line). The distance from the QCP for $CeIrIn_5$ is considered to be small since quantum critical behavior is observed below ~ 30 K. “B” is a crossover regime to a Fermi liquid (Ref. 18).

$\Gamma_a(\vec{Q}) < \Gamma_c(\vec{Q})$ has been confirmed for $CeIrIn_5$ at low temperatures. The dimensionality and the type of magnetic anisotropy are different concepts, and should be carefully distinguished in experiments aimed at determining the correlation between these attributes and superconductivity.

ACKNOWLEDGMENTS

We thank T. D. Matsuda and Y. Haga for preparation of high-quality single-crystal samples, as well as T. Takimoto, H. Adachi, K. Kubo, and H. Ikeda for stimulating discussions regarding the dynamical susceptibility. We are indebted to T. Takeuchi for communicating his unpublished specific-heat results for $LaIrIn_5$, which is used for the estimation of T_0 . This work was supported by a Grant-in-Aid for Scientific Research on Innovative Areas “Heavy Electrons” of the Ministry of Education, Culture, Sports, Science, and Technology, Japan.

¹J. Flouquet, *Progress in Low Temperature Physics*, edited by W. P. Halperin (Elsevier, New York, 2005), Vol. XV, p. 3.

²J. L. Sarrao and J. D. Thompson, *J. Phys. Soc. Jpn.* **76**, 051013 (2007).

³H. Hegger, C. Petrovic, E. G. Moshopoulou, M. F. Hundley, J. L. Sarrao, Z. Fisk, and J. D. Thompson, *Phys. Rev. Lett.* **84**, 4986 (2000).

⁴E. D. Bauer, D. Mixson, F. Ronning, N. Hur, R. Movshovich, J. D. Thompson, J. L. Sarrao, M. F. Hundley, P. H. Tobash, and S. Bobev, *Physica B* **378-380**, 142 (2006).

⁵L. D. Pham, T. Park, S. Maquilon, J. D. Thompson, and Z. Fisk, *Phys. Rev. Lett.* **97**, 056404 (2006).

⁶G.-q. Zheng, K. Tanabe, T. Mito, S. Kawasaki, Y. Kitaoka, D.

Aoki, Y. Haga, and Y. Ōnuki, *Phys. Rev. Lett.* **86**, 4664 (2001).

⁷W. Bao, G. Aeppli, J. W. Lynn, P. G. Pagliuso, J. L. Sarrao, M. F. Hundley, J. D. Thompson, and Z. Fisk, *Phys. Rev. B* **65**, 100505(R) (2002).

⁸S. Kambe, Y. Tokunaga, H. Sakai, H. Chudo, Y. Haga, T. D. Matsuda, and R. E. Walstedt, *Phys. Rev. B* **81**, 140405(R) (2010).

⁹C. Petrovic, R. Movshovich, M. Jaime, P. G. Pagliuso, M. F. Hundley, J. L. Sarrao, Z. Fisk, and J. D. Thompson, *Europhys. Lett.* **53**, 354 (2001).

¹⁰S. Kambe, H. Sakai, Y. Tokunaga, H. Kato, T. Fujimoto, R. E. Walstedt, S. Ikeda, T. D. Matsuda, Y. Haga, D. Aoki, Y. Homma, Y. Shiokawa, and Y. Ōnuki, *J. Magn. Magn. Mater.* **310**, 176

- (2007).
- ¹¹T. Takeuchi, T. Inoue, K. Sugiyama, D. Aoki, Y. Tokiwa, Y. Haga, K. Kindo, and Y. Ōnuki, *J. Phys. Soc. Jpn.* **70**, 877 (2001).
- ¹²Y. Haga, Y. Inada, H. Harima, K. Oikawa, M. Murakawa, H. Nakawaki, Y. Tokiwa, D. Aoki, H. Shishido, S. Ikeda, N. Watanabe, and Y. Ōnuki, *Phys. Rev. B* **63**, 060503(R) (2001).
- ¹³T. Moriya, *Prog. Theor. Phys.* **16**, 641 (1956).
- ¹⁴The off-diagonal term considered by N. J. Curro, J. L. Sarrao, J. D. Thompson, P. G. Pagliuso, S. Kos, A. Abanov, and D. Pines, for CeCoIn₅ [*Phys. Rev. Lett.* **90**, 227202 (2003)], is not taken into account since this contribution is usually quite small and cannot be determined in CeIrIn₅ since there is no magnetic ordered state.
- ¹⁵M. Yashima, H. Mukuda, Y. Kitaoka, H. Shishido, R. Settai, and Y. Ōnuki, *Phys. Rev. B* **79**, 214528 (2009).
- ¹⁶C. Stock, C. Broholm, J. Hudis, H. J. Kang, and C. Petrovic, *Phys. Rev. Lett.* **100**, 087001 (2008). The value of $\xi_{xy}/\xi_z \sim 2.5$ reported in this reference may be somewhat underestimated for our analysis since it is determined at a finite energy ~ 0.55 meV.
- ¹⁷Y. M. Ivanchenko and A. A. Lisyansky, *Physics of Critical Fluctuations* (Springer-Verlag, New York, 1995).
- ¹⁸S. Sachdev, *Quantum Phase Transitions* (Cambridge University Press, Cambridge, 1999).
- ¹⁹H. v. Löhneysen, A. Rosch, K. Vojta, P. Wölfle, *Rev. Mod. Phys.* **79**, 1015 (2007).
- ²⁰A. Abanov and A. Chubukov, *Phys. Rev. Lett.* **93**, 255702 (2004).
- ²¹T. Moriya and K. Ueda, *Rep. Prog. Phys.* **66**, 1299 (2003).
- ²²H. Shishido, R. Settai, D. Aoki, S. Ikeda, H. Nakawaki, N. Nakamura, T. Iizuka, Y. Inada, K. Sugiyama, T. Takeuchi, K. Kindo, T. C. Kobayashi, Y. Haga, H. Harima, Y. Aoki, T. Namiki, H. Sato, and Y. Ōnuki, *J. Phys. Soc. Jpn.* **64**, 960 (1995). The method for estimating T_0 is described in Ref. 29.
- ²³Y. Kuramoto and Y. Kitaoka, *Dynamics of Heavy Electrons* (Clarendon Press, Oxford, 2000).
- ²⁴S. Kambe, H. Sakai, Y. Tokunaga, T. Fujimoto, R. E. Walstedt, S. Ikeda, D. Aoki, Y. Homma, Y. Haga, Y. Shiokawa, and Y. Ōnuki, *Phys. Rev. B* **75**, 140509(R) (2007).
- ²⁵H. Kato, H. Sakai, Y. Tokunaga, Y. Tokiwa, S. Ikeda, Y. Ōnuki, S. Kambe, and R. E. Walstedt, *J. Phys. Soc. Jpn.* **72**, 2357 (2003).
- ²⁶H. Sakai, S. Kambe, Y. Tokunaga, T. Fujimoto, R. E. Walstedt, H. Yasuoka, D. Aoki, Y. Homma, E. Yamamoto, A. Nakamura, Y. Shiokawa, and Y. Ōnuki, *Phys. Rev. B* **76**, 024410 (2007).
- ²⁷R. Borth, E. Lengyel, P. G. Pagliuso, J. L. Sarrao, G. Sparn, F. Steglich, and J. D. Thompson, *Physica B* **312-313**, 136 (2002).
- ²⁸H. Sakai, S.-H. Baek, S. E. Brown, F. Ronning, E. D. Bauer, and J. D. Thompson, *Phys. Rev. B* **82**, 020501(R) (2010).
- ²⁹S. Kambe, J. Flouquet, and T. E. Hargreaves, *J. Low Temp. Phys.* **108**, 383 (1997).